

Component mode synthesis methods using partial interface modes: Application to tuned and mistuned structures with cyclic symmetry

Duc-Minh Tran

► **To cite this version:**

Duc-Minh Tran. Component mode synthesis methods using partial interface modes: Application to tuned and mistuned structures with cyclic symmetry. *Computers and Structures*, Elsevier, 2009, 87 (17-18), pp.1141-1153. 10.1016/j.compstruc.2009.04.009 . hal-01537665

HAL Id: hal-01537665

<https://hal.archives-ouvertes.fr/hal-01537665>

Submitted on 12 Jun 2017

HAL is a multi-disciplinary open access archive for the deposit and dissemination of scientific research documents, whether they are published or not. The documents may come from teaching and research institutions in France or abroad, or from public or private research centers.

L'archive ouverte pluridisciplinaire **HAL**, est destinée au dépôt et à la diffusion de documents scientifiques de niveau recherche, publiés ou non, émanant des établissements d'enseignement et de recherche français ou étrangers, des laboratoires publics ou privés.



Component mode synthesis methods using partial interface modes: Application to tuned and mistuned structures with cyclic symmetry

Duc-Minh Tran

ONERA, The French Aerospace Lab, Aeroelasticity and Structural Dynamics Department, B.P. 72, 29 Avenue de la Division Leclerc, 92322 Châtillon Cedex, France

We present new component mode synthesis methods using partial interface modes which are the structure normal modes resulting from the static condensation of the structure to the interface between the substructures and which are possibly clamped at a part of this interface. These methods are the generalization of the classical component mode synthesis methods and those using the interface modes. These methods allow to reduce the number of the interface coordinates and at the same time to keep some of the physical interface displacements. These methods are applied to a structure with cyclic symmetry in both tuned and mistuned cases.

Keywords:
Component mode synthesis
Dynamic substructuring
Interface mode
Partial interface mode
Cyclic symmetry
Mistuning

1. Introduction

Component mode synthesis (CMS) or dynamic substructuring methods consist in performing the dynamic analysis of structures by decomposing the structure into substructures and by projecting the equation of motion of each substructure on a projection basis to obtain the reduced systems of the substructures before performing the substructure coupling to obtain the reduced system of the whole structure. In the classical CMS methods, the substructure projection basis is composed, on one hand, by the normal modes of the substructure with various boundary conditions at the interface, such as fixed interface [18,19,36,39,40], free interface [3,14,18,20,32,36,37,49,50,61], hybrid interface [20,28,49,73,74], or loaded interface [6], and on the other hand, by Ritz vectors derived from the static deformation shapes commonly called the static modes, such as the constraint modes, the attachment modes, the residual attachment modes etc. CMS methods have been described in several text books [5,31,41,52,54], many insights, variants and improvements have been proposed [1,8,23,26,27,29,38,42–46,48,56,58–60,64,66,69–71], and CMS methods have been widely used for a large range of applications [4,7,9,10,15–17,22,24,30,35,47,51,53,55,62,63,65,67,76–80]. A history, review and classification of CMS methods can be found in [25].

In the classical CMS methods, the generalized coordinates associated with the static modes are in most of the cases the

displacements at the interface between the substructures, leading to reduced systems with large size due to the important number of degrees of freedom (DOF) at the interface. In order to reduce the number of interface DOF, the CMS methods using interface modes has first been developed for the fixed interface CMS method [2,12,13,21] and then extended to the free and hybrid interface CMS methods [72]. In these methods, the static modes are replaced by the interface modes, also called the junction modes or the eigen modes of the Poincaré–Steklov operator, which are the first few normal modes of the whole structure after performing the Guyan static condensation [33] to the interface between the substructures. The interface displacements associated with the static modes in the classical CMS methods are then replaced by a few generalized coordinates associated with the interface modes. Alternative approaches for reducing the interface DOF were also proposed in [2,11,21,34].

Although the CMS methods using interface modes produce reduced systems with very small size, one drawback is that all the interface DOF are removed from the reduced system. The presence of a part of the interface DOF in the reduced system is however sometimes desirable and even essential, either because these DOF are not numerous and they can provide quick and useful information, or because one needs to deal directly with them while solving the reduced system, for example to impose prescribed motions or to take into account local non-linearities such as contact, friction or free-play. The aim of this paper, which is a continuation of the work in [72], is to develop new CMS methods using partial interface modes which fix this drawback. These methods allow at the same time an important reduction of the number of the

interface DOF like in the CMS methods using interface modes, and the conservation of some interface DOF in the reduced system like in the classical CMS methods. To reach this aim, the approach in this work is that, instead of computing the interface modes, the latter are approximated by applying a second level CMS method on Guyan's reduced system resulting from the static condensation of the whole structure to the interface between the substructures. The DOF of Guyan's reduced system are partitioned into two sets containing respectively the interface DOF to be eliminated and those to be kept in the final reduced system, the former being considered as the interior DOF and the latter as the interface DOF in the second level CMS method. The choice of the kept interface DOF depends on the need of the user to keep them in the reduced system. The partial interface modes are defined as a first few normal modes of Guyan's reduced system in which some of the kept interface DOF can be clamped, depending upon which CMS method, i.e. with fixed, free or hybrid interface, is applied to Guyan's reduced system. The partial interface modes are completed with the static modes of Guyan's reduced system, whose associated generalized coordinates are precisely the kept interface DOF, and together they replace the interface modes or the substructure static modes in the projection basis. The classical methods and the methods using interface modes are particular cases of the new methods using partial interface modes, the former are obtained when all the interface DOF are kept, and the latter when all the interface DOF are eliminated.

This paper is organized as follows: In Section 2, the classical CMS methods and the methods using interface modes are reminded. In Section 3, the new CMS methods using partial interface modes are presented. Section 4 deals with the case of structures with cyclic symmetry. In Section 5, the new CMS methods are applied to compute the eigen frequencies and modes and the frequency response of a tuned and mistuned bladed disk, with several selections of partial interface modes and kept interface DOF. They are compared with the whole structure computations and also with the classical methods and the methods using interface modes.

2. Classical methods and methods using interface modes

2.1. Substructure description, reduced system and coupling

We consider a structure S which is decomposed into n_s substructures S_j ($j = 1, \dots, n_s$) which do not overlap. We denote by L^S the part of S which consists in the frontier between the substructures and by L_j the frontier of S_j with the adjacent substructures. L^S and L_j will be called the interface of S and S_j . The interface L^S is partitioned into L_k^S , the interface DOF to be kept in the final reduced coupled system, and L_e^S , the interface DOF to be eliminated. The number of DOF in L_k^S is very small compared to the number of DOF in L_e^S . The kept interface L_k^S is then partitioned into the fixed interface L_{ck}^S and the free kept interface L_{ak}^S .

For each substructure S_j , the interface L_j is also partitioned into the fixed interface L_c and the free interface L_a , thus L_j can be fixed ($L_a = \emptyset$ and $L_c = L_j$), free ($L_c = \emptyset$ and $L_a = L_j$) or hybrid ($L_c \neq \emptyset$, $L_a \neq \emptyset$, $L_j = L_c \cup L_a$), in the latter case S_j is supposed to be constrained when L_c is fixed. The choice of L_c and L_a can be different from one substructure to another, and it is completely independent of the choice of L_{ck}^S and L_{ak}^S .

The vectors of the physical displacements of S , L^S , L_e^S , L_k^S , L_{ck}^S , L_{ak}^S , S_j , L_j , L_c and L_a are respectively \mathbf{x}^S , \mathbf{x}_L^S , $\mathbf{x}_{L_e}^S$, $\mathbf{x}_{L_k}^S$, $\mathbf{x}_{L_{ck}}^S$, $\mathbf{x}_{L_{ak}}^S$, \mathbf{x} , \mathbf{x}_L , \mathbf{x}_{L_c} and \mathbf{x}_{L_a} . Let us define the boolean matrices \mathbf{P}_S^L which restricts \mathbf{x}^S to \mathbf{x} , \mathbf{P}_L^L which restricts \mathbf{x}_L^S to \mathbf{x}_L , and \mathbf{P}_L , \mathbf{P}_c and \mathbf{P}_a which restrict \mathbf{x} to \mathbf{x}_L , \mathbf{x}_{L_c} and \mathbf{x}_{L_a} respectively: $\mathbf{x} = \mathbf{P}_S^L \mathbf{x}^S$, $\mathbf{x}_L = \mathbf{P}_L^L \mathbf{x}_L^S = \mathbf{P}_L \mathbf{x}$, $\mathbf{x}_{L_c} = \mathbf{P}_c \mathbf{x}$ and $\mathbf{x}_{L_a} = \mathbf{P}_a \mathbf{x}$.

The equilibrium equation of the isolated substructure S_j is written as:

$$\mathbf{K}\mathbf{x} + \mathbf{C}\dot{\mathbf{x}} + \mathbf{M}\ddot{\mathbf{x}} = \mathbf{f}_e - {}^t\mathbf{P}_L \mathbf{f}_L. \quad (1)$$

\mathbf{K} , \mathbf{C} and \mathbf{M} are the stiffness, damping and mass matrices of S_j , \mathbf{f}_e are the external forces applied on S_j and \mathbf{f}_L are the interface reactions exerted by S_j on L_j . The left superscript ${}^t(\cdot)$ denotes the transpose of a vector or a matrix.

The CMS methods consist in expressing the displacements of the substructure as a linear combination of the Ritz vectors in a projection basis \mathbf{Q} , i.e. $\mathbf{x} = \mathbf{Q}\mathbf{q}$, where \mathbf{q} is the vector of the generalized coordinates. By projecting the equilibrium equation (1) on the projection basis \mathbf{Q} , we obtain a reduced system:

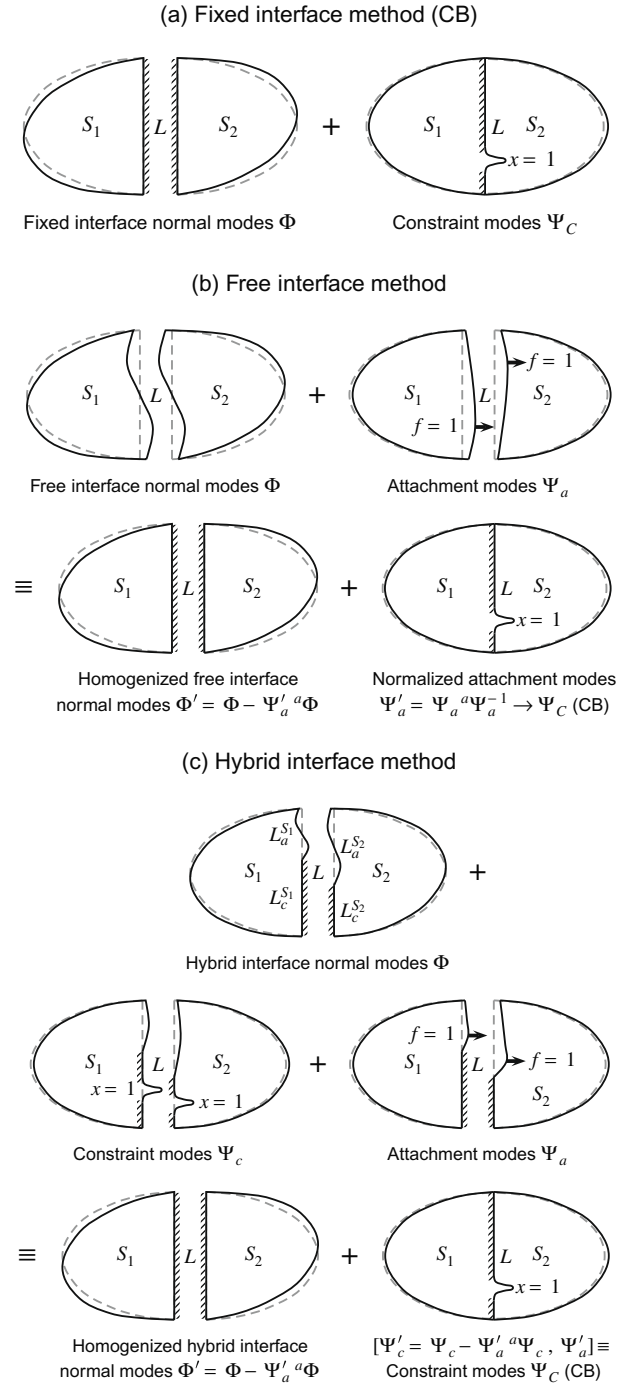


Fig. 1. Classical CMS methods.

$${}^t\mathbf{Q}\mathbf{K}\mathbf{Q}\mathbf{q} + {}^t\mathbf{Q}\mathbf{C}\mathbf{Q}\dot{\mathbf{q}} + {}^t\mathbf{Q}\mathbf{M}\mathbf{Q}\ddot{\mathbf{q}} = {}^t\mathbf{Q}\mathbf{f}_e - {}^t\mathbf{Q}{}^t\mathbf{P}_L\mathbf{f}_L. \quad (2)$$

The coupling of the substructures is fairly simple, it is performed by using the continuity of the interface displacements and the equilibrium of the interface reactions. It corresponds to the primal coupling formulation described in [25] which consists in assembling the substructure reduced matrices to form the reduced matrices of the whole structure, similarly to the assembly of the elementary matrices in the finite-element procedure. In the assembled reduced matrices, the substructure reduced matrices are coupled through the interface generalized coordinates which are at least common to two substructures, such as the interface displacements or the generalized coordinates associated with the interface modes or the partial interface modes.

2.2. Classical CMS methods

In the classical hybrid interface methods using attachment modes [28,72,74], the displacements of S_j are expressed as (Fig. 1c):

$$\begin{aligned} \mathbf{x} &= (\Phi - \Psi_a^a \Phi) \boldsymbol{\mu} + (\Psi_c - \Psi_a^a \Psi_c) \mathbf{x}_{Lc} + \Psi_a^a \mathbf{x}_{La} \\ &= \Phi' \boldsymbol{\mu} + \Psi_c^c \mathbf{x}_{Lc} + \Psi_a^a \mathbf{x}_{La}, \end{aligned} \quad (3)$$

where the left superscripts $a(\cdot) = \mathbf{P}_a(\cdot)$ and $c(\cdot) = \mathbf{P}_c(\cdot)$ denote the restrictions to the free interface L_a and the fixed interface L_c ; Φ are the hybrid interface normal modes of S_j , i.e. with L_c fixed and L_a free; Ψ_c are the constraint modes obtained by imposing unit displacements on L_c and with L_a free; Ψ_a are the attachment modes obtained by applying opposite of unit forces on L_a and with L_c fixed; $\Psi_a^a = \Psi_a^a \Psi_a^{-1}$ are the normalized attachment modes; $\Psi_c^c = \Psi_c - \Psi_a^a \Psi_c$ are the homogenized constraint modes; and $\Phi' = \Phi - \Psi_a^a \Phi$ are the homogenized normal modes. We have: ${}^a\Psi_a^a = \mathbf{I}$, ${}^c\Psi_a^a = \mathbf{0}$, ${}^a\Psi_c^c = \mathbf{0}$, ${}^c\Psi_c^c = \mathbf{I}$, ${}^a\Phi' = \mathbf{0}$ and ${}^c\Phi' = \mathbf{0}$.

The Craig and Bampton (CB) classical fixed interface method [19] (Fig. 1a) is a particular case of Eq. (3) in which Ψ_a and Ψ_a^a do not exist, $\Phi' = \Phi$ are the fixed interface normal modes, and $\Psi_c^c = \Psi_c = \Psi_c$, where Ψ_c are the constraint modes of the CB method.

The classical free interface method using the attachment modes [36,74] (Fig. 1b) is also a particular case of Eq. (3) in which Ψ_c and Ψ_c^c do not exist, Φ are the free interface normal modes. For unconstrained substructures, the rigid body modes should be included in Φ , and a special treatment should be used when computing Ψ_a , which consists in balancing the applied unit forces with the inertia forces and in orthogonalizing the static solutions to the rigid body modes [72].

It has been showed in [72] that in the hybrid interface methods, the Ritz vectors $[\Psi_c^c, \Psi_a^a]$ associated with the interface displacements in Eq. (3) are exactly the constraint modes Ψ_c of the CB method. In the free interface method, Ψ_a^a are equal to Ψ_c for constrained substructures, while for unconstrained substructures a variant can be obtained by replacing Ψ_a^a by Ψ_c . By using this variant of the free interface method, Eq. (3) can be written for the three types of interface as:

$$\mathbf{x} = \Phi' \boldsymbol{\mu} + \Psi_c^c \mathbf{x}_L. \quad (4)$$

The reduced system Eq. (2) is obtained by projecting Eq. (1) on the projection basis $\mathbf{Q} = [\Phi', \Psi_c^c]$, the unknowns are the modal coordinates $\boldsymbol{\mu}$ and the interface displacements \mathbf{x}_L , and the substructure coupling is performed through \mathbf{x}_L .

Some variants [49,61,73,74] use the residual attachment modes $\Psi_{ar} = \Psi_a + \Phi({}^t\Phi\mathbf{K}\Phi)^{-1}{}^t\Phi$ instead of the attachment modes. Although the attachment modes and the residual attachment modes should theoretically give the same results since the two sets $[\Phi, \Psi_a]$ and $[\Phi, \Psi_{ar}]$ span the same subspace, the redundant contribution of Φ in Ψ_a being simply removed in Ψ_{ar} , it is easier

to compute Ψ_a than Ψ_{ar} , and the inversion of ${}^a\Psi_{ar}$ for obtaining Ψ_{ar} is subjected to numerical problems since the terms of ${}^a\Psi_{ar}$ are very small when the number of the normal modes retained in Φ is important. Moreover, contrarily to the attachment modes, the residual attachment modes do not satisfy the relationships $\Psi_{ar} = \Psi_c$ for the free interface method and $[\Psi_c^c, \Psi_{ar}^a] = \Psi_c$ for the hybrid interface method.

2.3. CMS methods using interface modes

At the whole structure level, the displacements of S are expressed from Eq. (4) as:

$$\mathbf{x}^S = \Phi^S \boldsymbol{\mu}^S + \Psi_c^S \mathbf{x}_L^S, \quad (5)$$

where the homogenized normal modes Φ^S and the constraint modes Ψ_c^S of S are the extensions of the substructure homogenized normal modes Φ and constraint modes Ψ_c to S by completing with zeros on the other substructures. Ψ_c^S are also the global constraint modes of S obtained by imposing unit displacements on L^S .

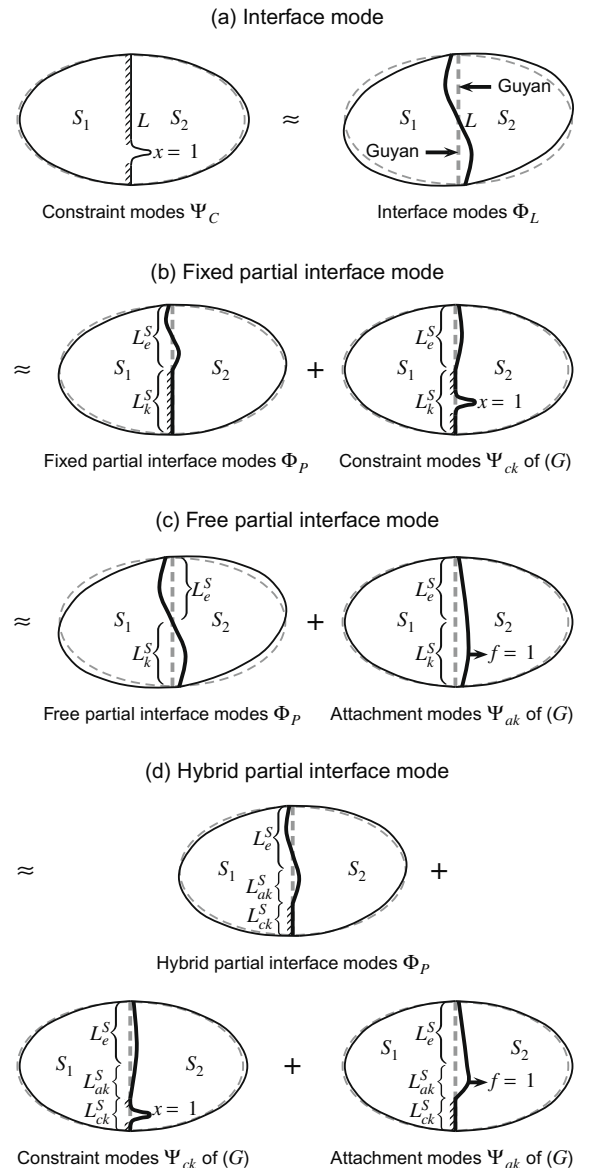


Fig. 2. CMS methods using interface modes and partial interface modes. (G) is Guyan's reduced system Eq. (6).

In order to reduce the number of interface DOF, the constraint modes Ψ_C^S in Eq. (5) are replaced by the interface modes which are obtained by performing Guyan's static condensation of the whole structure S on the interface L^S , i.e. by expressing the displacements of S as $\mathbf{x}^S = \Psi_C^S \mathbf{x}_L^S$. By projecting the free equation of motion of S on Ψ_C^S , we obtain Guyan's reduced system:

$$\mathbf{K}_L^S \mathbf{X}_L^S = \mathbf{M}_L^S \mathbf{X}_L^S \Omega_L^2, \quad (6)$$

with $\mathbf{K}_L^S = {}^t \Psi_C^S \mathbf{K}^S \Psi_C^S$ and $\mathbf{M}_L^S = {}^t \Psi_C^S \mathbf{M}^S \Psi_C^S$, \mathbf{K}^S and \mathbf{M}^S being the stiffness and mass matrices of S .

The interface modes are the eigen vectors \mathbf{X}_L^S of Guyan's reduced system Eq. (6). The structure interface modes Φ_L^S are the approximated normal modes of S obtained by the expansion of \mathbf{X}_L^S to S using Ψ_C^S , and the substructure interface modes Φ_L of S_j are the restriction of Φ_L^S to S_j (Fig. 2a):

$$\Phi_L^S = \Psi_C^S \mathbf{X}_L^S \quad \text{and} \quad \Phi_L = \mathbf{P}_{S_j}^L \Phi_L^S = \Psi_C^j \mathbf{X}_L^S, \quad (7)$$

where the left superscript $j(\cdot) = \mathbf{P}_{S_j}^L(\cdot)$ denotes the restriction to the interface L_j .

In practice, the interface modes are computed by projecting the stiffness and mass matrices of S_j on Ψ_C and then by assembling the resulting reduced matrices to obtain the reduced system Eq. (6), like in the CB method but without the normal modes Φ . Since the whole set of all the structure interface modes Φ_L^S and the structure constraint modes Ψ_C^S span the same subspace, a truncation of the subspace spanned by Ψ_C^S is obtained by keeping among the solutions of Eq. (6) only the few interface modes \mathbf{X}_L^S , Φ_L^S and Φ_L corresponding to the lowest frequencies in Ω_L .

The CMS method using interface modes [12,21,72] consists in replacing the constraint modes Ψ_C^S by the interface modes Φ_L^S in Eq. (5), which is the same as replacing the constraint modes Ψ_C by the interface modes Φ_L in Eq. (4). The physical displacements of S_j are expressed as:

$$\mathbf{x} = \Phi' \boldsymbol{\mu} + \Phi_L \boldsymbol{\mu}_L. \quad (8)$$

The generalized coordinates $\boldsymbol{\mu}_L$ are not associated with any particular substructure, they are in contrary common to all the substructures. The reduced system of S_j is obtained by projecting Eq. (1) on the projection basis $\mathbf{Q} = [\Phi', \Phi_L]$ and the substructure coupling is performed through the interface coordinates $\boldsymbol{\mu}_L$. Eq. (8) provides reduced coupled systems with a much smaller size than Eqs. (3) and (4), which however do not contain any interface displacements of \mathbf{x}_L and \mathbf{x}_L^S .

3. CMS methods using partial interface modes

In the classical CMS methods or the methods using interface modes, the interface displacements \mathbf{x}_L^S are either kept or eliminated in their totality in the final reduced coupled system. If we want to keep the displacements of the interface L_k^S and eliminate those of L_e^S , the idea is to replace the interface modes by another set of vectors whose some of the associated generalized coordinates are precisely the displacements $\mathbf{x}_{L_k}^S$ of L_k^S . To this aim, we consider Guyan's reduced system Eq. (6) as the free equation of motion of a structure whose DOF are the displacements \mathbf{x}_L^S of L^S . We can then apply again a second level CMS method to Eq. (6) by considering L_e^S as the interior DOF and L_k^S as the interface DOF. The partial interface modes are the normal modes of Eq. (6) which are possibly clamped at a part of the kept interface L_k^S , depending upon which CMS method, i.e. with fixed, free or hybrid interface, is applied to Eq. (6). These partial interface modes are completed with the static modes of Eq. (6) associated with L_e^S , both sets are then expanded to the whole structure and then restricted to the substructures in order to form the projection basis of the substructure displacements. This

approach is similar to the Ritz reduction of junction coordinates described in [21], where the Ritz vectors were however not specified in the general case and they were obtained from analytical functions in an application.

For instance, if the hybrid interface method given in Eq. (3) is applied to Guyan's reduced system Eq. (6), the kept interface L_k^S is partitioned into the fixed kept interface L_{ck}^S and the free kept interface L_{ak}^S . The hybrid partial interface modes \mathbf{X}_p^S are the normal modes of Guyan's reduced system Eq. (6) with hybrid interface, i.e. with L_{ck}^S fixed and L_{ak}^S free, while the constraint modes \mathbf{X}_{ck}^S of Eq. (6) are obtained by imposing unit displacements on L_{ck}^S and with L_{ak}^S free, and the attachment modes \mathbf{X}_{ak}^S of Eq. (6) are obtained by applying opposite of unit forces on L_{ak}^S and with L_{ck}^S fixed (Fig. 2d). Similarly to Eq. (3), the interface modes \mathbf{X}_L^S of Eq. (6) are then expressed as:

$$\mathbf{X}_L^S = \mathbf{X}_p^{Sr} \mathbf{B} + \mathbf{X}_{ck}^{Sr} \mathbf{X}_L^S + \mathbf{X}_{ak}^{Sr} \mathbf{X}_L^S, \quad (9)$$

where the superscripts $k(\cdot)$, $ck(\cdot)$ and $ak(\cdot)$ denote the restrictions to L_k^S , L_{ck}^S and L_{ak}^S ; \mathbf{B} are the generalized coordinates; $\mathbf{X}_{ak}^{Sr} = \mathbf{X}_{ak}^{S(ak\mathbf{X}_{ak}^S)^{-1}}$ are the normalized attachment modes; $\mathbf{X}_p^{Sr} = \mathbf{X}_p^S - \mathbf{X}_{ak}^{Sr} \mathbf{X}_p^S$ are the homogenized partial interface modes, i.e. the homogenized hybrid interface normal modes; and $\mathbf{X}_{ck}^{Sr} = \mathbf{X}_{ck}^S - \mathbf{X}_{ak}^{Sr} \mathbf{X}_{ck}^S$ are the homogenized constraint modes of Eq. (6). Since ${}^k \mathbf{X}_p^{Sr} = \mathbf{0}$, ${}^{ck} \mathbf{X}_{ck}^{Sr} = \mathbf{I}$, ${}^{ak} \mathbf{X}_{ak}^{Sr} = \mathbf{0}$, ${}^{ck} \mathbf{X}_{ak}^{Sr} = \mathbf{0}$ and ${}^{ak} \mathbf{X}_{ak}^{Sr} = \mathbf{I}$, it is clear that the generalized coordinates associated with \mathbf{X}_{ck}^{Sr} and \mathbf{X}_{ak}^{Sr} in Eq. (9) are the restrictions ${}^{ck} \mathbf{X}_L^S$ and ${}^{ak} \mathbf{X}_L^S$ of \mathbf{X}_L^S to L_{ck}^S and L_{ak}^S respectively.

In order to build the reduced systems of the substructures, we only need the homogenized partial interface modes Φ'_p , the homogenized constraint modes Ψ'_{ck} and the normalized attachment modes Ψ'_{ak} of S_j . They are obtained in the same way as in Eq. (7), by the expansion using Ψ_C^{Sr} of \mathbf{X}_p^{Sr} , \mathbf{X}_{ck}^{Sr} and \mathbf{X}_{ak}^{Sr} to S to obtain Φ_p^{Sr} , Ψ'_{ck} and Ψ'_{ak} , and by the restriction of the latter to S_j :

$$\Phi_p^{Sr} = \Psi_C^{Sr} \mathbf{X}_p^{Sr}, \quad \Psi'_{ck} = \Psi_C^{Sr} \mathbf{X}_{ck}^{Sr}, \quad \Psi'_{ak} = \Psi_C^{Sr} \mathbf{X}_{ak}^{Sr}, \quad (10)$$

$$\Phi'_p = \Psi_C^j \mathbf{X}_p^{Sr}, \quad \Psi'_{ck} = \Psi_C^j \mathbf{X}_{ck}^{Sr}, \quad \Psi'_{ak} = \Psi_C^j \mathbf{X}_{ak}^{Sr}. \quad (11)$$

Since the expansion using Ψ_C^{Sr} of L^S to the whole structure keeps the displacements at L^S unchanged, we have: ${}^k \Phi_p^{Sr} = \mathbf{0}$, ${}^{ck} \Psi'_{ck} = \mathbf{I}$, ${}^{ak} \Psi'_{ak} = \mathbf{0}$, ${}^{ck} \Psi'_{ak} = \mathbf{0}$ and ${}^{ak} \Psi'_{ck} = \mathbf{I}$. From Eqs. (7) and (9), the interface modes of S and S_j become:

$$\Phi_L^S = \Psi_C^S \mathbf{X}_L^S = \Phi_p^{Sr} \mathbf{B} + \Psi'_{ck} \mathbf{X}_L^S + \Psi'_{ak} \mathbf{X}_L^S, \quad (12)$$

$$\Phi_L = \Psi_C^j \mathbf{X}_L^S = \Phi'_p \mathbf{B} + \Psi'_{ck} \mathbf{X}_L^S + \Psi'_{ak} \mathbf{X}_L^S. \quad (13)$$

In practice, the partial interface modes \mathbf{X}_p^S , the constraint modes \mathbf{X}_{ck}^S and the attachment modes \mathbf{X}_{ak}^S of Guyan's reduced system Eq. (6) are computed, as well as \mathbf{X}_p^{Sr} , \mathbf{X}_{ck}^{Sr} and \mathbf{X}_{ak}^{Sr} , with a special treatment for \mathbf{X}_{ak}^S if the whole structure is unconstrained. Only Φ'_p , Ψ'_{ck} and Ψ'_{ak} are then deduced by using Eq. (11).

The CMS method using hybrid partial interface modes consists in replacing the constraint modes Ψ_C^S by the interface modes Φ_L^S given by Eq. (12) in Eq. (5), which is the same as substituting the expression Eq. (13) of the interface modes Φ_L in Eq. (8). The displacements of the substructure S_j are expressed as:

$$\mathbf{x} = \Phi' \boldsymbol{\mu} + \Phi'_p \boldsymbol{\mu}_p + \Psi'_{ck} \mathbf{x}_{L_{ck}}^S + \Psi'_{ak} \mathbf{x}_{L_{ak}}^S. \quad (14)$$

Since ${}^k \Phi_p^{Sr} = \mathbf{0}$ and from the above values of Φ_p^{Sr} , Ψ'_{ck} and Ψ'_{ak} at the kept interface L_k^S , L_{ck}^S and L_{ak}^S , the generalized coordinates associated with Ψ'_{ck} and Ψ'_{ak} in Eq. (14) are respectively the physical displacements $\mathbf{x}_{L_{ck}}^S$ and $\mathbf{x}_{L_{ak}}^S$ of the fixed and the free kept interfaces L_{ck}^S and L_{ak}^S , and they are common to all the substructures (see Remark 1). The reduced system of S_j is obtained by projecting Eq. (1) on the projection basis $\mathbf{Q} = [\Phi', \Phi'_p, \Psi'_{ck}, \Psi'_{ak}]$. The substructure coupling is performed through the interface coordinates $\boldsymbol{\mu}_p$ and the kept interface displacements $\mathbf{x}_{L_{ck}}^S$ and $\mathbf{x}_{L_{ak}}^S$, which are now part of the unknowns in the reduced coupled system.

Table 1
Formulations of CMS methods.

Number	Method	Type of interface	Formulation
<i>Classical CMS methods, Eq. (3)</i>			
1	CB	Fixed interface [19]	$\mathbf{x} = \Phi\boldsymbol{\mu} + \Psi_c\mathbf{x}_L$
2	FA	Free interface [36]	$\mathbf{x} = \Phi'\boldsymbol{\mu} + \Psi'_a\mathbf{x}_L$, with $\Psi'_a = \Psi_a^a\Psi_a^{-1}$ and $\Phi' = \Phi - \Psi_a^a\Phi$
3	HA	Hybrid interface [28]	$\mathbf{x} = \Phi'\boldsymbol{\mu} + \Psi'_c\mathbf{x}_{Lc} + \Psi'_a\mathbf{x}_{La}$, with $\Psi'_c = \Psi_c - \Psi_a^a\Psi_c$
<i>Variants using Ψ_c of classical CMS methods, Eq. (4)</i>			
4	FA'	Free interface [72]	$\mathbf{x} = \Phi'\boldsymbol{\mu} + \Psi_c\mathbf{x}_L$ (identical to FA if constrained substructure)
5	HA'	Hybrid interface [72]	$\mathbf{x} = \Phi'\boldsymbol{\mu} + \Psi_c\mathbf{x}_L$ (identical to HA)
<i>CMS methods with interface modes (I), Eq. (8)</i>			
6	CBI	Fixed interface [12,21]	$\mathbf{x} = \Phi\boldsymbol{\mu} + \Phi_L\boldsymbol{\mu}_L$
7	FAI	Free interface [72]	$\mathbf{x} = \Phi'\boldsymbol{\mu} + \Phi_L\boldsymbol{\mu}_L$
8	HAI	Hybrid interface [72]	$\mathbf{x} = \Phi'\boldsymbol{\mu} + \Phi_L\boldsymbol{\mu}_L$
<i>CMS methods with fixed partial interface modes (PCB), Eq. (15)</i>			
9	CBPCB	Fixed interface	$\mathbf{x} = \Phi\boldsymbol{\mu} + \Phi_p\boldsymbol{\mu}_p + \Psi_{ck}\mathbf{x}_{Lk}^S$
10	FAPCB	Free interface	$\mathbf{x} = \Phi'\boldsymbol{\mu} + \Phi_p\boldsymbol{\mu}_p + \Psi_{ck}\mathbf{x}_{Lk}^S$
11	HAPCB	Hybrid interface	$\mathbf{x} = \Phi'\boldsymbol{\mu} + \Phi_p\boldsymbol{\mu}_p + \Psi_{ck}\mathbf{x}_{Lk}^S$
<i>CMS methods with free partial interface modes (PFA), Eq. (16)</i>			
12	CBPFA	Fixed interface	$\mathbf{x} = \Phi\boldsymbol{\mu} + \Phi_p\boldsymbol{\mu}_p + \Psi'_{ak}\mathbf{x}_{Lk}^S$, with $\Phi'_p = \Phi_p - \Psi'_{ak}\mathbf{x}_p^S$
13	FAPFA	Free interface	$\mathbf{x} = \Phi'\boldsymbol{\mu} + \Phi_p\boldsymbol{\mu}_p + \Psi'_{ak}\mathbf{x}_{Lk}^S$
14	HAPFA	Hybrid interface	$\mathbf{x} = \Phi'\boldsymbol{\mu} + \Phi_p\boldsymbol{\mu}_p + \Psi'_{ak}\mathbf{x}_{Lk}^S$
<i>CMS methods with hybrid partial interface modes (PHA), Eq. (14)</i>			
15	CBPHA	Fixed interface	$\mathbf{x} = \Phi\boldsymbol{\mu} + \Phi_p\boldsymbol{\mu}_p + \Psi'_{ck}\mathbf{x}_{Lck}^S + \Psi'_{ak}\mathbf{x}_{Lak}^S$
16	FAPHA	Free interface	$\mathbf{x} = \Phi'\boldsymbol{\mu} + \Phi_p\boldsymbol{\mu}_p + \Psi'_{ck}\mathbf{x}_{Lck}^S + \Psi'_{ak}\mathbf{x}_{Lak}^S$
17	HAPHA	Hybrid interface	$\mathbf{x} = \Phi'\boldsymbol{\mu} + \Phi_p\boldsymbol{\mu}_p + \Psi'_{ck}\mathbf{x}_{Lck}^S + \Psi'_{ak}\mathbf{x}_{Lak}^S$

If the fixed interface method ($L_{ck}^S = L_k^S$, $L_{ak}^S = \emptyset$) or the free interface method ($L_{ak}^S = L_k^S$, $L_{ck}^S = \emptyset$) is applied to Guyan's reduced system Eq. (6), we obtain the CMS method using fixed partial interface modes (Fig. 2b) or the CMS method using free partial interface modes (Fig. 2c). Eq. (14) becomes respectively:

$$\mathbf{x} = \Phi'\boldsymbol{\mu} + \Phi_p\boldsymbol{\mu}_p + \Psi_{ck}\mathbf{x}_{Lk}^S, \quad (15)$$

$$\mathbf{x} = \Phi'\boldsymbol{\mu} + \Phi_p\boldsymbol{\mu}_p + \Psi'_{ak}\mathbf{x}_{Lk}^S. \quad (16)$$

Eq. (16) is an improved variant of the CMS method using interface modes given by Eq. (8), since the free partial interface modes Φ_p are exactly the interface modes Φ_L , while the attachment modes Ψ_{ak} represent a static correction to the truncation of the interface modes. In some cases however, the free partial interface modes Φ_p are not the same as the interface modes Φ_L , for example when the cyclic symmetry properties are used in combination with the CMS methods.

The formulations of all CMS methods are summarized in Table 1.

3.1. Remarks

- (1) All the DOF of the kept interface L_k^S , i.e. \mathbf{x}_{Lk}^S , are involved in the expressions Eqs. (14)–(16) of the displacements of the substructure S_j , and not only the DOF of L_k^S who belong to S_j , even when S_j does not contain any DOF of L_k^S . Since the constraint modes Ψ_{ck}^S , Ψ_{ck} and the attachment modes Ψ_{ak}^S , Ψ_{ak} result from the deformations of the whole structure S under the solicitations applied or imposed on L_{ck}^S or L_{ak}^S , a substructure S_j can be deformed even if the solicitations are not applied or imposed on its interface, except when all of its interface DOF are fixed like in the constraint modes Ψ_c of the CB method.
- (2) The CMS methods using partial interface modes are the generalization of the classical methods and the methods using interface modes. Indeed, if all the interface displacements are eliminated in the reduced system, i.e. $L_k^S = \emptyset$ and $L_e^S = L^S$, we obtain the methods using interface modes given by Eq. (8). On the other hand, if all the interface displacements are kept in the reduced system, i.e. $L_k^S = L^S$ and $L_e^S = \emptyset$, we obtain the classical methods given by Eq. (4).

- (3) If all the interface modes or all the partial interface modes of Guyan reduced system Eq. (6) are kept in \mathbf{X}_L^S and \mathbf{X}_p^S , i.e. if no truncation is made on these sets, the methods using interface modes and partial interface modes should provide the same results as the classical methods given by Eq. (4). Otherwise, the methods using interface modes and partial interface modes are less accurate than the classical methods. With the same number of interface modes and partial interface modes, the latter are expected to provide better results than the former, since the static modes of Guyan's reduced system represent a static correction to the truncation of the interface modes.
- (4) Unlike in the classical Guyan static condensation where the choice of the master and the slave DOF is made without a clear criterion, the choice of the kept interface DOF L_k^S , and by consequent of the eliminated interface DOF L_e^S , depends only on the need of the user to keep them in the reduced system. The methods using partial interface modes should therefore be considered as an improvement of the methods using interface modes which, beside the reduction of the size of the reduced system, offers the possibility to keep some interface DOF in the latter. Also unlike in Guyan's condensation where an important number of the master DOF should be kept to obtain good results, the presence of only a few interface DOF in the reduced system is sufficient to improve significantly the accuracy and the convergence of the results over the methods using interface modes, with only a small additional computation cost, as it will be showed in the numerical example. Therefore, even in the case the interface DOF are not needed in the reduced system, it is better to keep some of them and use the partial interface modes rather than the interface modes.

4. Case of structures with cyclic symmetry

A structure with cyclic symmetry is composed of N identical sectors S_0, S_1, \dots, S_{N-1} , it is obtained by $N - 1$ repeated rotations of the reference sector S_0 through the angle $\alpha = 2\pi/N$ rd to form

a circular system. The reference sector S_0 has a right frontier L_r and a left frontier L_l with the adjacent sectors. Using the cyclic symmetry properties [68,75], only the reference sector S_0 is modeled and N systems of equations of S_0 in the complex traveling wave coordinates $\mathbf{x}^{S_0,n}$ are solved for N phase numbers $n = 0, \dots, N-1$ (or N phase angles $\alpha_n = n\alpha$), with appropriate second members and by imposing the cyclic symmetry boundary conditions [72]:

$$\mathbf{x}_{L_l}^{S_0,n} = \mathbf{x}_{L_r}^{S_0,n} e^{i\alpha_n}. \quad (17)$$

In order to reduce the size of the system of equations of S_0 , the CB method has been used in [35], and the classical free and hybrid interface methods as well as the methods using interface modes in [72]. This section describes how the methods using partial interface modes can be used in combination with the cyclic symmetry properties, however it is also applicable for the classical methods and the methods using interface modes.

The reference sector S_0 being decomposed into substructures (but not necessarily), the interface L^{S_0} of S_0 is composed of the frontiers L_r , L_l and the interface between the substructures composing S_0 . L^{S_0} is then partitioned into the kept interface L_k and the eliminated interface L_e . Let us define the kept right frontier $L_{rk} = L_r \cap L_k$, the kept left frontier $L_{lk} = L_l \cap L_k$, the eliminated right frontier $L_{re} = L_r \cap L_e$ and the eliminated left frontier $L_{le} = L_l \cap L_e$. We impose the condition that L_{rk} and L_{lk} should correspond to the same DOF on L_r and L_l , and by consequent L_{re} and L_{le} also verify the same condition. The kept interface L_k is partitioned into the fixed kept interfaces L_{ck} and the free kept interfaces L_{ak} , without any condition.

At first, we compute the normal modes Φ (with fixed, free or hybrid interface), the constraint modes Ψ_c and Ψ_C , and the attachment modes Ψ_a of the isolated substructures composing S_0 , without using the cyclic symmetry conditions.

Guyan's reduced system Eq. (6) of the reference sector S_0 is then formed by projecting the stiffness and mass matrices of the substructures on their constraint modes Ψ_C and by coupling the substructure reduced matrices, or equivalently, by projecting the matrices \mathbf{K}^{S_0} and \mathbf{M}^{S_0} of S_0 on its constraint modes $\Psi_C^{S_0}$:

$$\mathbf{K}_L \mathbf{X}_L = \mathbf{M}_L \mathbf{X}_L \Omega^2, \quad (18)$$

with $\mathbf{K}_L = {}^t \Psi_C^{S_0} \mathbf{K}^{S_0} \Psi_C^{S_0}$ and $\mathbf{M}_L = {}^t \Psi_C^{S_0} \mathbf{M}^{S_0} \Psi_C^{S_0}$.

From Eq. (18), we compute the partial interface modes \mathbf{X}_p^n , the constraint modes \mathbf{X}_{ck}^n and the attachment modes \mathbf{X}_{ak}^n . Since they are the modes of the whole structure, the cyclic symmetry boundary conditions Eq. (17) are applied, but uniquely on the eliminated right and left frontiers L_{re} and L_{le} at this stage, as if the sectors are only connected at these frontiers:

$$\mathbf{x}_{L_{le}}^{S_0,n} = \mathbf{x}_{L_{re}}^{S_0,n} e^{i\alpha_n}. \quad (19)$$

The normalized attachment modes $\mathbf{X}_{ak}^{nv} = \mathbf{X}_{ak}^n (\mathbf{X}_{ak}^n)^{-1}$, the homogenized partial interface modes $\mathbf{X}_p^{nv} = \mathbf{X}_p^n - \mathbf{X}_{ak}^{nv} \mathbf{X}_p^n$ and the homogenized constraint modes $\mathbf{X}_{ck}^{nv} = \mathbf{X}_{ck}^n - \mathbf{X}_{ak}^{nv} \mathbf{X}_{ck}^n$ are then computed, from which we deduce the homogenized partial interface modes Φ_p^{nv} , the homogenized constraint modes Ψ_{ck}^{nv} and the normalized attachment modes Ψ_{ak}^{nv} of the substructures composing S_0 by using Eq. (11):

$$\Phi_p^{nv} = \Psi_C^j \mathbf{X}_p^{nv}, \quad \Psi_{ck}^{nv} = \Psi_C^j \mathbf{X}_{ck}^{nv}, \quad \Psi_{ak}^{nv} = \Psi_C^j \mathbf{X}_{ak}^{nv}. \quad (20)$$

From Eq. (14), the displacements of the substructures composing S_0 are expressed in the traveling wave coordinates as:

$$\mathbf{x}^n = \Phi' \mu^n + \Phi_p^{nv} \mu_p^{S_0,n} + [\Psi_{ck}^{nv}, \Psi_{ak}^{nv}] \mathbf{x}_{L_k}^{S_0,n}, \quad (21)$$

where Φ' are the homogenized normal modes which do not depend on n , μ^n and $\mu_p^{S_0,n}$ are the complex generalized coordinates, $\mathbf{x}_{L_k}^{S_0,n}$ are the complex displacements of the kept interface L_k of S_0 . Note that

μ^n are associated to only one substructure, while $\mu_p^{S_0,n}$ and $\mathbf{x}_{L_k}^{S_0,n}$ are common to all the substructures composing S_0 .

The displacements $\mathbf{x}^{S_0,n}$ of S_0 resulting from the expression Eq. (21) of the substructure displacements \mathbf{x}^n already verified the cyclic symmetry boundary conditions Eq. (19) on the eliminated right and left frontiers L_{re} and L_{le} , since $\Phi_{L_{re}}^{S_0'} = \Phi_{L_{le}}^{S_0'} = \mathbf{0}$, and $\Phi_p^{S_0,nv}$, $\Psi_{ck}^{S_0,nv}$ and $\Psi_{ak}^{S_0,nv}$ already verified Eq. (19).

The reduced systems of the substructures are obtained by projecting the equilibrium equation of the substructures on the projection basis $\mathbf{Q}^n = [\Phi', \Phi_p^{nv}, \Psi_{ck}^{nv}, \Psi_{ak}^{nv}]$. The coupling of the substructure reduced systems through the generalized coordinates $\mu_p^{S_0,n}$ and the kept interface displacements $\mathbf{x}_{L_k}^{S_0,n}$ provides the reduced system of S_0 whose unknowns are $\mathbf{q}^{S_0,n} = {}^t [\mu_p^{S_0,n}, \mathbf{x}_{L_k}^{S_0,n}]$, where $\mu_p^{S_0,n}$ contains the generalized coordinates μ^n of all the substructures composing S_0 . The coupled reduced system is solved by applying the cyclic symmetry conditions Eq. (17) on the kept right and left frontiers L_{rk} and L_{lk} :

$$\mathbf{K}_R^{S_0,n} \mathbf{q}^{S_0,n} + \mathbf{C}_R^{S_0,n} \dot{\mathbf{q}}^{S_0,n} + \mathbf{M}_R^{S_0,n} \ddot{\mathbf{q}}^{S_0,n} = \mathbf{f}_R^{S_0,n} + \mathbf{f}_{LR}^{S_0,n}, \quad (22)$$

$$\mathbf{x}_{L_k}^{S_0,n} = \mathbf{x}_{L_{rk}}^{S_0,n} e^{i\alpha_n}. \quad (23)$$

The solutions of Eqs. (22) and (23) provide the generalized coordinates $\mathbf{q}^{S_0,n}$ from which the traveling wave coordinates \mathbf{x}^n of the substructures and $\mathbf{x}^{S_0,n}$ of S_0 are deduced by using Eq. (21). The real physical displacements of each sector S_j are obtained as the real part of a summation on $\mathbf{x}^{S_0,n}$: $\mathbf{x}^j = \Re \left\{ \sum_{n=0}^{N-1} \mathbf{x}^{S_0,n} e^{ij\alpha_n} \right\}$.

Let us notice that the cyclic symmetry boundary conditions Eq. (17) are applied in two stages, at first on the eliminated left and right frontiers L_{re} and L_{le} in Eq. (19) when computing the partial interface modes and the static modes of Guyan's reduced system Eq. (18), and secondly on the kept left and right frontiers L_{rk} and L_{lk} in Eq. (23) when solving the reduced system Eq. (22) of S_0 .

In two particular cases, the cyclic symmetry conditions are imposed only once on the whole frontiers L_r and L_l : (i) when solving the reduced coupled system Eq. (22) in the classical methods where $L_e = \emptyset$, since there is no interface modes or partial interface modes [35]; and (ii) when solving Guyan's reduced system Eq. (18) in the methods using interface modes where $L_k = \emptyset$, since there is no physical interface DOF in Eq. (22) [72].

Moreover, the free partial interface modes are computed by imposing the cyclic symmetry conditions on the eliminated frontiers L_{re} and L_{le} in Guyan's reduced system, so they are different to the interface modes for which these conditions are imposed on L_r and L_l . These two sets will be the same if all the DOF of L_r and L_l are eliminated, i.e. if $L_r \subset L_e$ and $L_l \subset L_e$.

5. Numerical application

5.1. Test case description and computation cases

The structure S consists of a cyclically symmetric bladed disk (Fig. 3a) which is composed of 15 repetitive sectors with data given in Table 2. The structure is clamped on the inner circle, so the DOF on the latter will not be taken into account. The number of DOF of the whole structure S is 10350 (3 DOF per node, only the flexural motion is considered).

At first, we consider the tuned case where only the reference sector S_0 is modeled. For the CMS methods, S_0 is decomposed into two substructures, the reference disk sector D_0 and the reference blade B_0 (Fig. 3b). The interface L^{S_0} of S_0 , which is also the interface L^{D_0} of D_0 , is composed of the right frontier L_r , the left frontier L_l and the disk-blade interface L^{B_0} . The numbers of DOF of S_0 , D_0 , B_0 , L^{S_0} , L_r , L_l and L^{B_0} are respectively 750, 660, 99, 129, 60, 60 and 9.

In a second stage, we introduce a mistuning in the structure, which consists in the random coefficients c_{ki} and c_{mi} for

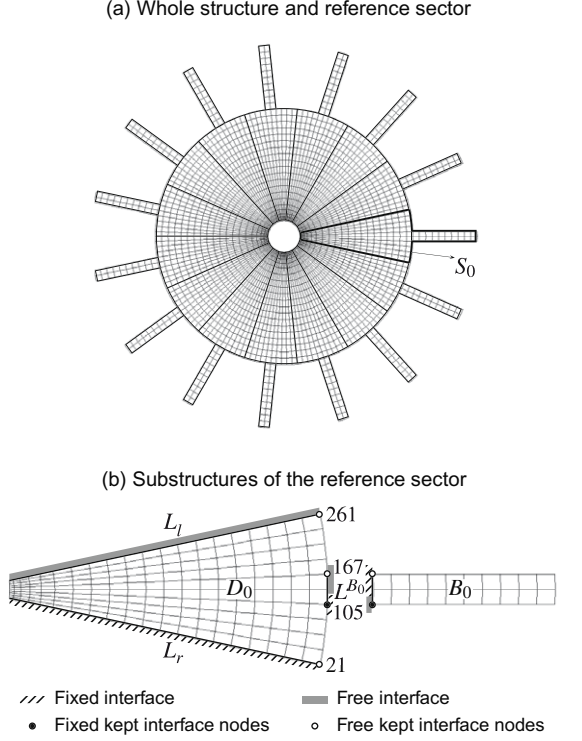


Fig. 3. Structure, reference sector and decomposition into substructures.

Table 2

Bladed disk data.

Inner radius of the disk	12.7×10^{-3} m
Outer radius of the disk	101.6×10^{-3} m
Outer radius of the bladed disk	152.4×10^{-3} m
Blade length	50.8×10^{-3} m
Blade width	8.5×10^{-3} m
Thickness	1.982×10^{-3} m
Young's modulus	2×10^{11} N/m ²
Poisson's ratio	0.3
Density	7860 kg/m ³

$i = 0, \dots, 14$, with mean value 1 and standard deviation 0.2 (Table 3). The stiffness and mass matrices of the mistuned structure are obtained by multiplying the stiffness matrix of the tuned sector S_i by c_{ki} and the mass matrix of S_i by c_{mi} . For the CMS methods, the structure is decomposed into 30 substructures, 15 disk sectors and 15 blades (Fig. 3a). The number of DOF of the interface L^S between the substructures is 1035. Two approaches are used, in the first one (MIS1) the projection bases, i.e. the substructure normal and static modes and the interface modes or partial interface modes, are computed from the mistuned structure, while in the second one (MIS2) they are computed from the tuned structure. The advantage of the second approach is that the normal modes and the static modes of the tuned reference disk sector D_0 and blade B_0 are used for all the substructures, and the tuned interface modes and partial interface modes can be computed by using the cyclic symmetry properties.

Table 3

Coefficients for mistuning.

S_i	0	1	2	3	4	5	6	7	8	9	10	11	12	13	14
c_{ki}	0.88	0.80	1.19	0.61	1.12	1.25	1.27	1.13	0.89	0.93	0.74	1.03	0.81	1.25	1.09
c_{mi}	0.91	1.20	0.79	0.94	1.36	1.15	0.74	1.28	1.10	0.68	0.74	1.08	1.10	0.88	1.05

The results of the CMS methods are compared to the reference results obtained by using the cyclic symmetry (CS) without CMS for the tuned case, and by performing the computations on the whole structure (WS) for the mistuned cases.

5.2. Component mode synthesis methods

The CMS methods used in the numerical application are organized into three groups, in each group the same type of interface (fixed, free or hybrid) is used for both substructure modes and partial interface modes: the fixed interface group (CB); the free interface using attachment modes group (FA); and the hybrid interface using attachment modes group (HA). Other combinations such as the CB method with free or hybrid partial interface modes are of course possible, but they are not used here since the number of the considered CMS methods is already too important.

In each group, we consider three methods (Table 1):

- the classical method (CB, FA and HA, or C in short) and the variants using Ψ_C of the free and hybrid interface classical methods (FA' and HA', or C' in short);
- the method using interface modes (CBI, FAI and HAI);
- the method using partial interface modes (CBP, FAP and HAP, number 9, 13 and 17 in Table 1), with two selections of the kept interface DOF (Fig. 3b). In the first selection P1, nodes 105 and 167 on the disk-blade interface L^{B_0} are kept in the reduced system. In the second selection P2, nodes 105, 167 and also nodes 21, 261 on the left and right frontiers of S_0 are kept. The numbers of the kept interface DOF are respectively 6 and 12 in the tuned case. The same selections are made for the other sectors with the corresponding nodes in the mistuned case, the numbers of the kept interface DOF are respectively 90 and 135 for P1 and P2.

In the hybrid interface group (HA), the following choice of the fixed interface and the free interface is made in the tuned case (Fig. 3b): concerning the substructure modes, L_r and node 105 are fixed (L_l and the other nodes of L^{B_0} are free) for D_0 , while 105 is free (the other nodes of L^{B_0} are fixed) for B_0 ; concerning the partial interface modes, node 105 is fixed while nodes 21, 167 and 261 are free. The same choice is made for the other disk sectors D_i , blades B_i and sectors S_i with the corresponding nodes in the mistuned case. The above choice is made so that not only the substructures have the hybrid interface, but the substructure coupling is also performed between the fixed interface and the free interface.

5.3. Mode selections

We are interested to the eigen frequencies of the structure up to $f_{\max} = 3000$ Hz. For the substructure normal modes, we use Rubin's criterion [61] which consists in selecting all the free interface normal modes whose frequencies are smaller than a cut-out frequency defined by $f_{cs} = 1.5f_{\max} = 4500$ Hz. In the tuned case, five modes are selected for the disk sector D_0 and four modes for the blade B_0 , including three rigid body modes for the latter (Fig. 4). The same numbers of modes are used for the fixed and hybrid interface modes, and also in the mistuned case for each disk sector D_i and each blade B_i .

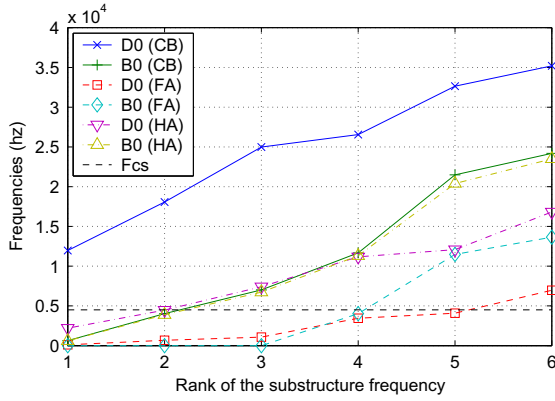


Fig. 4. Frequencies of the substructures D_0 and B_0 with fixed (CB), free (FA) and hybrid (HA) interface in the tuned case.

A similar criterion is used with a different cut-out frequency $f_{ci} = c_i f_{max}$ for the interface modes and the partial interface modes [72] (Fig. 5). Three selections (a, b and c) are used, corresponding respectively to $c_i = 1.5, 2.5$ and 3.5 ($f_{ci} = 4500, 7500$ and $10,500$ Hz). In order to select the same number of interface modes and partial interface modes for all the methods, the maximum number of modes given by the criterion is used for each selection. They are respectively 4, 5 and 6 in the tuned case for each phase number, and 44, 62, 81 in the mistuned case. A suffix (for instance CBlA, CBP1b) indicates which selection is used.

Figs. 4 and 5 show that the frequencies of the substructure and partial interface modes in the CB and HA cases (fixed and hybrid interface) are much higher than those in the FA case (free interface). If we apply Rubin's criterion to the CB and HA cases with the same cut-out frequency, the number of the selected modes will

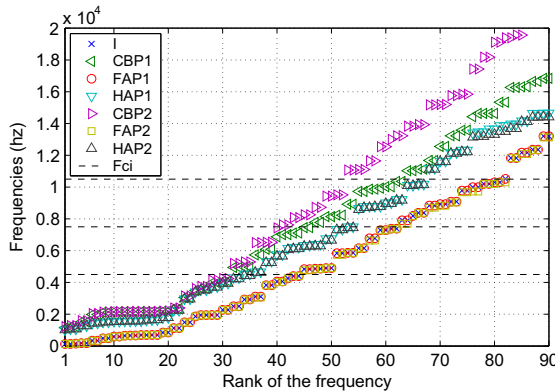


Fig. 5. Frequencies of the interface mode (I) and the partial interface modes (P1 and P2) with fixed (CB), free (FA) and hybrid (HA) interface in the tuned case.

Table 4

Size of the assembled reduced system and mean adimensioned CPU time (reduction and solution) of the frequency response.

Method	Reference CS, WS	Classical C, C'	Interface mode			Partial interface mode					
			la	lb	lc	P1a	P1b	P1c	P2a	P2b	P2c
<i>Size of the assembled reduced system</i>											
Tuned	750	138	13	14	15	19	20	21	25	26	27
Mistuned	10,350	1170	179	197	216	269	287	306	314	332	351
<i>Mean CPU time (adimensioned by the smallest value, 3.26 s)</i>											
Tuned	328.6	46.3	1	1.1	1.3	1.2	1.3	1.4	3.0	3.3	3.6
MIS1	765.7	166.9	11.7	14.6	17.3	30.5	35.4	40.0	42.2	47.4	53.3
MIS2		161.6	6.7	9.9	12.5	24.8	31.2	35.3	35.8	44.7	48.8

be very small. As Rubin's criterion was initially used in [61] to select the free interface substructure modes, we apply the criterion first to the FA case, and then use the same number of the selected modes for the CB and HA cases.

The size of the system in the reference cases CS and WS and the size of the coupled reduced system in all the CMS methods are given in Table 4.

5.4. Undamped frequencies and modes

The 40 frequencies of the structure up to 3000 Hz obtained in the reference CS and WS case are plotted in Fig. 6 for both tuned and mistuned cases. The tuned frequencies are double for the phase numbers $n \neq 0$. The mistuned frequencies are no longer double, however they are very close to those of the tuned case. The difference between the frequencies of the tuned and mistuned cases are comprised between $\pm 8\%$. The results of the CMS methods are not plotted since they are not distinguishable from the reference results.

Fig. 7 shows the relative errors on each frequency obtained with CMS methods and with Selection (a) of interface modes or partial interface modes. The classical methods give the smallest errors which are practically zeros, while the methods using interface modes give largest errors. As usually observed with CMS and other projection methods, the results are excellent on the low frequencies and deteriorate when the frequencies go up, due to the truncation of the projection basis. The truncation effect is emphasized after the 30th modes where the errors increase rapidly, in particular for the methods using interface modes.

Fig. 8 shows the evolution of the mean relative errors on the frequencies and modes obtained with the CMS methods using interface modes and partial interface modes in function of the number of the selected modes, the first three values corresponding

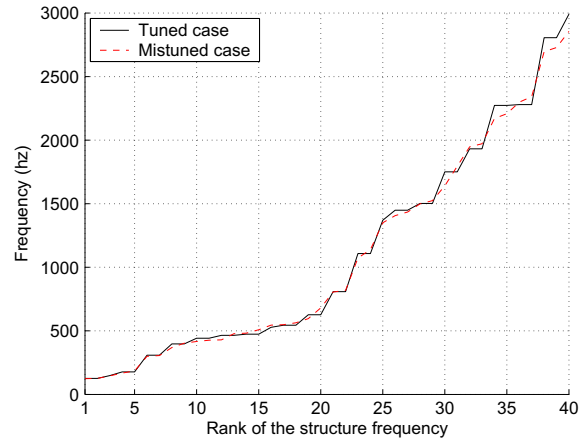


Fig. 6. Structure frequencies obtained in reference cases (CS and WS).

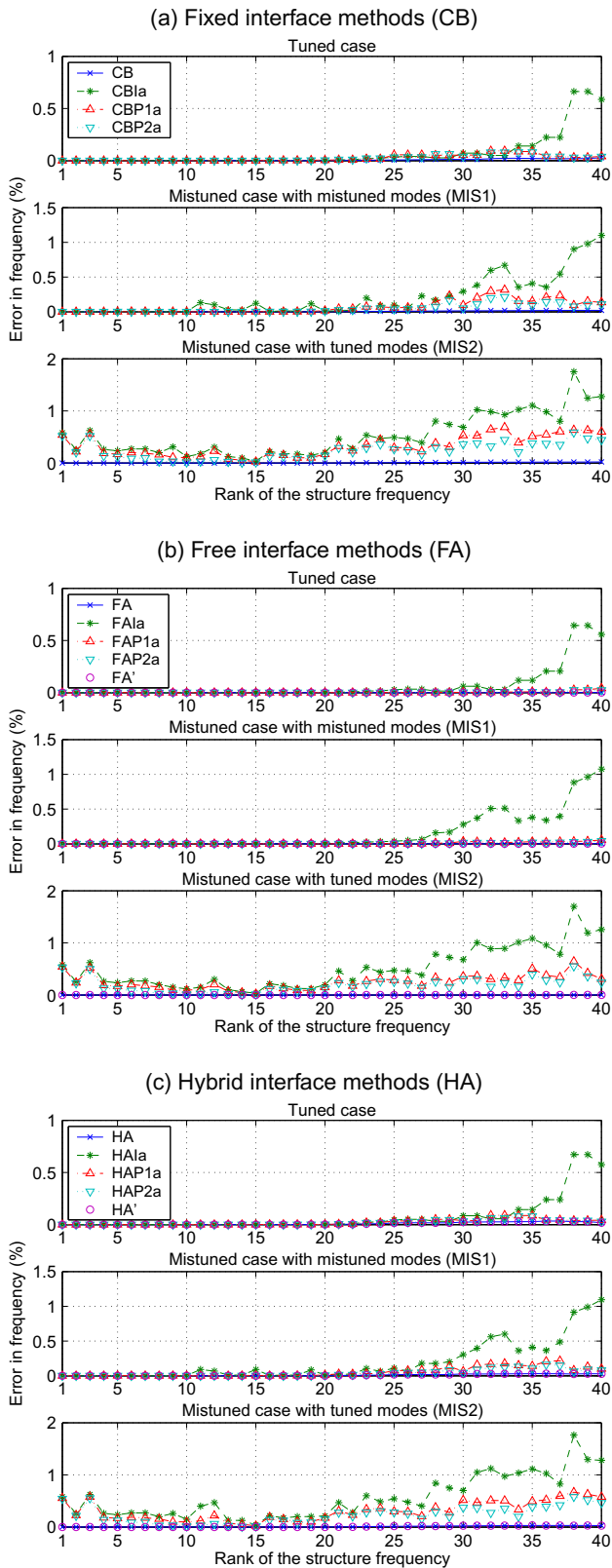


Fig. 7. Percent errors in frequency obtained with CMS methods.

to the mode selections (a–c) derived from Rubin’s criterion. The errors on the mode \mathbf{x}_i , normalized so that $\|\mathbf{x}_i\| = 1$, are obtained by $\varepsilon_i = \|\mathbf{x}_{i(\text{cms})} - (\mathbf{x}_{i(\text{ref})} \mathbf{x}_{i(\text{cms})}) \mathbf{x}_{i(\text{ref})}\| = \sqrt{1 - (\mathbf{x}_{i(\text{ref})} \mathbf{x}_{i(\text{cms})})^2}$. The three mode selections (a–c) provide very good results, for both interface

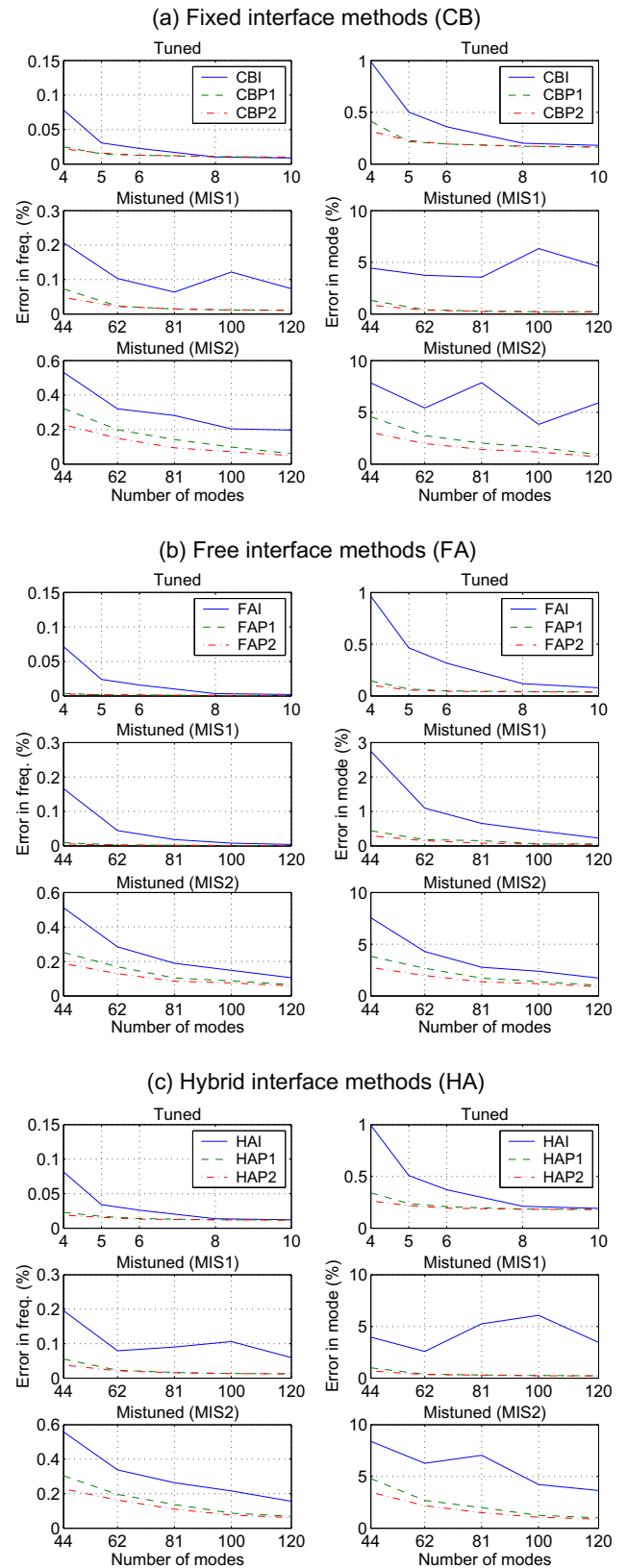


Fig. 8. Variation of mean errors in frequency and mode in function of the number of interface modes and partial interface modes.

modes and partial interface modes. Using more modes than in Selection (c) only improves slightly the results. With the same number of modes, the methods using interface modes are less

accurate than those using partial interface modes, as expected. The partial interface modes improve not only the accuracy of the results, but also their convergence when the number of modes increases. Indeed, the interface modes, although provide very good results, do not converge very well in the mistuned cases, except with the free interface method. Selection P2 provides better results than Selection P1 but not that much, despite that the number of the kept interface DOF is multiplied by 2 in the tuned case and by 1.5 in the mistuned case.

Fig. 9 shows the mean relative errors on the frequencies and modes obtained with all the CMS methods. For all the CMS methods, the results in the tuned case are much better than those in the mistuned cases, probably because the projection bases in the tuned case are more appropriate than in the mistuned case, since Rubin's criterion is used to select the substructure modes in the tuned case, and the same numbers of modes are then kept for the mistuned cases. The MIS1 mistuned case gives much better results than the MIS2 mistuned case, this means that the tuned projection bases do not represent the mistuned structure as accurately as the mistuned projection bases. The mean errors in the tuned, MIS1 and MIS2 cases are respectively smaller than 0.08%, 0.2% and 0.6% on the frequencies, and 1%, 6% and 8% on the modes. The classical methods provide the best results, with less than 0.02% mean error on the frequencies and less than 0.3% mean error on the modes. The variants FA' and HA' give the same results than the FA and HA methods. This confirms that the Ritz vectors associated with the interface DOF in the free and hybrid interface classical methods are either identical to or can be replaced by the constraint modes of the CB methods, and justifies the replacement

of the latter by the interface modes or the partial interface modes as in the CB method. The free interface methods are more accurate than the fixed interface and the hybrid interface methods, and the latter give similar results.

5.5. Frequency response to harmonic forces

Three harmonic forces, $f_1 = 10 \cos \Omega t - 10 \sin \Omega t$, $f_2 = 20 \cos \Omega t - 20 \sin \Omega t$ and $f_3 = 30 \cos \Omega t - 30 \sin \Omega t$, are applied to the DOF u_z of nodes 21, 105 and 261 of sector S_0 (Fig. 3b). A proportional damping matrix $\mathbf{C} = a\mathbf{K} + b\mathbf{M}$ is introduced, with $a = 5 \times 10^{-5}$ and $b = 1$. The frequency response is computed for both tuned and mistuned cases with the excitation frequency Ω varying from 2 to 1000 Hz with a step of 2 Hz.

Fig. 10 shows the frequency response of the amplitudes U_z of the displacements $u_z = U_z \cos(\Omega t + \varphi)$ of node 105 obtained in the reference cases (CS and WS). Three main resonance peaks are observed before 200 Hz, with a slight shift of the peaks towards the smaller frequencies in the mistuned case. The peak amplitudes are also a little different between the tuned and mistuned cases.

Fig. 11 shows the absolute errors $U_{z(\text{cms})} - U_{z(\text{ref})}$ obtained with the CMS methods and with Selection (a) of interface modes or partial interface modes. All the CMS methods give excellent amplitudes in the tuned and the MIS1 mistuned cases, the absolute errors are smaller than 10^{-6} , i.e. 4 order smaller than the amplitude. The results are less accurate in the MIS2 mistuned case, with absolute errors smaller than 10^{-3} .

Fig. 12 shows the relative errors on the amplitudes U_z which are defined as the ratio of the euclidian norms $\|\mathbf{U}_{z(\text{cms})} - \mathbf{U}_{z(\text{ref})}\| / \|\mathbf{U}_{z(\text{ref})}\|$, where \mathbf{U}_z is the vector containing the amplitudes U_z for all the excitation frequencies. All the CMS methods provide excellent results with relative errors smaller than 0.03%, 0.05% and 6% for the tuned, MIS1 and MIS2 cases respectively. Like in the frequency and mode computations, the classical methods and their variants are the most accurate. With the same mode selection (a-c), the methods using partial interface modes are more accurate than those using interface modes, and the accuracy increases with the number of interface modes and partial interface modes. Selection P2 of the kept interface DOF is only slightly better than Selection P1, and the free interface methods are better than the fixed and hybrid interface methods, but only in the tuned and MIS1 mistuned cases.

The mean CPU times, adimensioned by their smallest values 3.26 s, are presented in Table 4. For the CMS methods, the CPU time includes, on the one hand, the model reduction, i.e. the

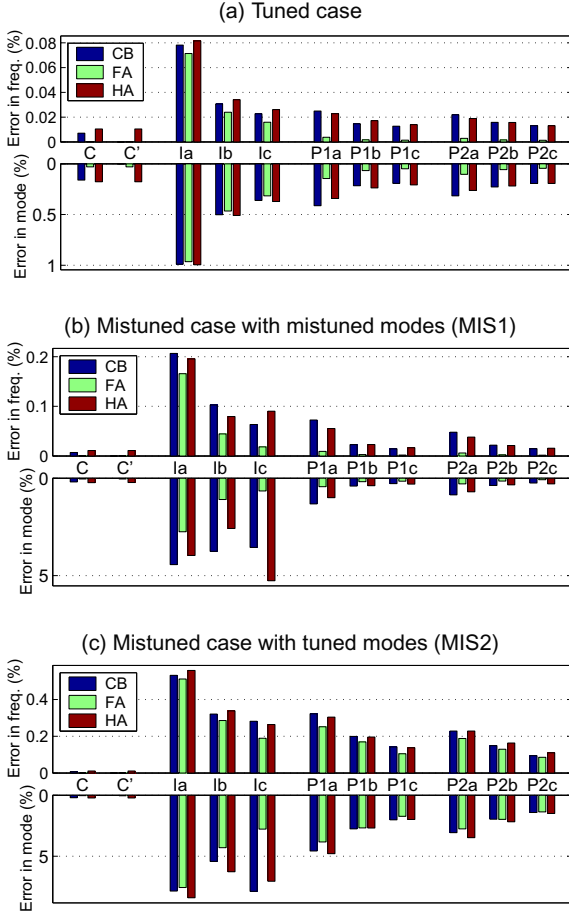


Fig. 9. Mean errors in frequency and mode obtained with CMS methods.

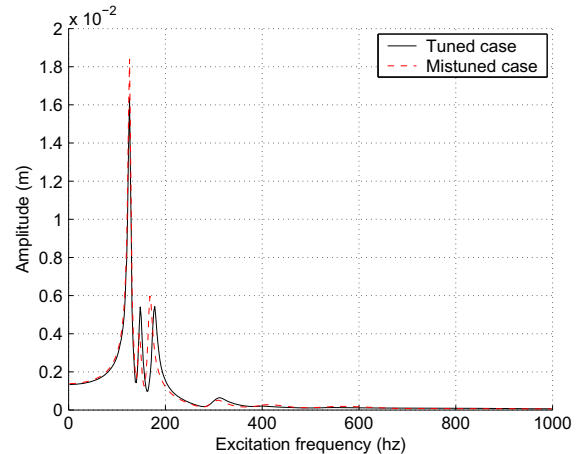


Fig. 10. Amplitude U_z obtained in reference cases (CS and WS).

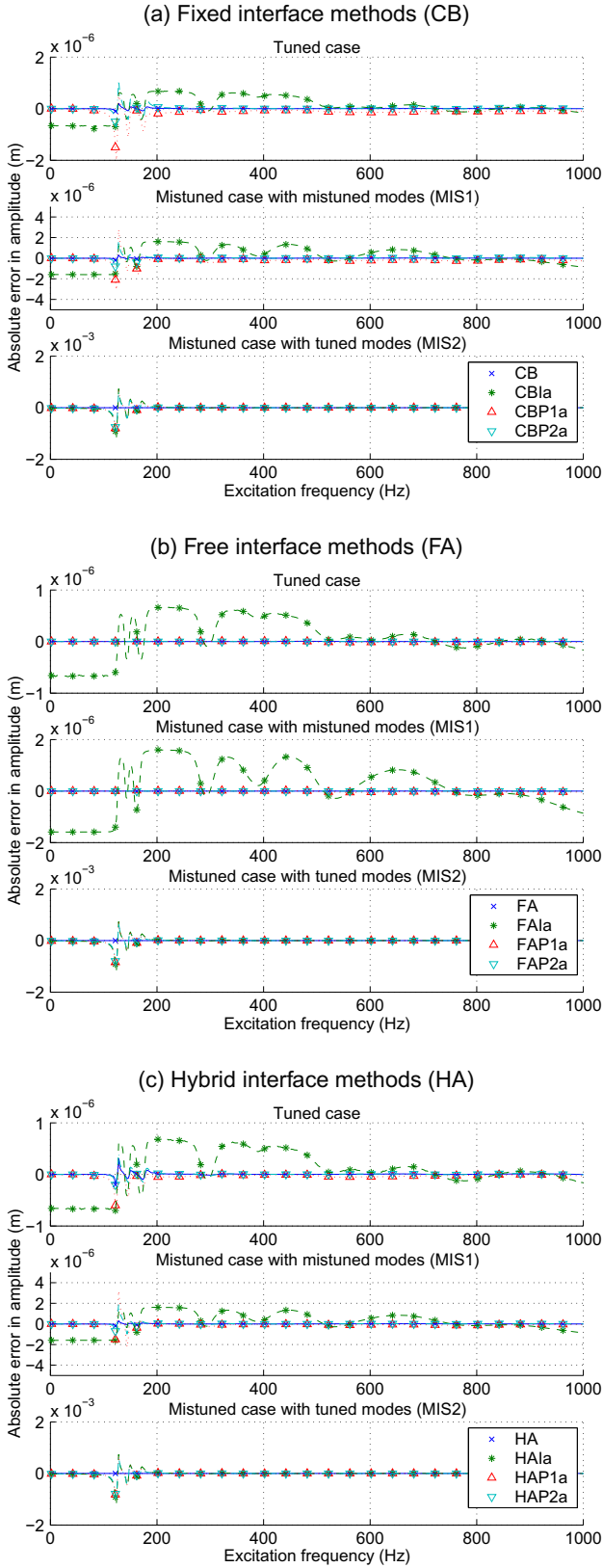


Fig. 11. Absolute errors in amplitude obtained with CMS methods.

computation of the substructure, interface and partial interface modes, the projection and the coupling of the substructures, and, on the other hand, the solution of the reduced system, including the restitution of the physical displacements.

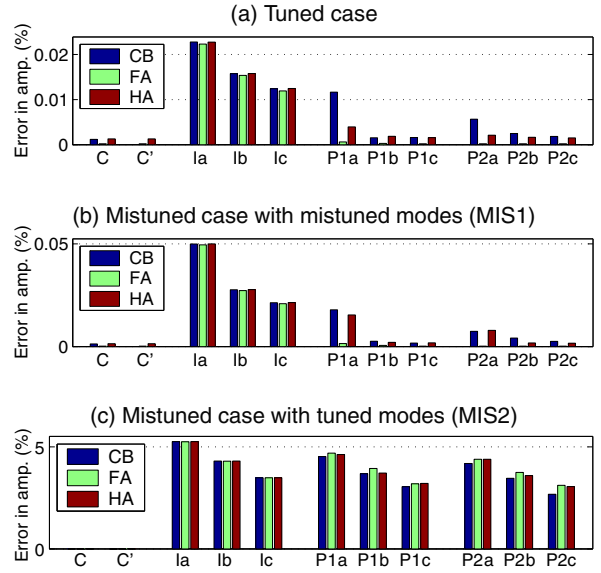


Fig. 12. Percent errors in amplitude obtained with CMS methods.

Thanks to the use of the cyclic symmetry properties, the CPU times of the tuned case compared to the mistuned cases is reduced in average by a factor of 2.3, 3.5, 10.6 and 17.1 respectively with the reference methods, the classical CMS methods, the methods using interface modes and the methods using partial interface modes. The CMS methods using interface modes and partial interface modes are in average 40 and 20 times faster than the classical methods in the tuned case, 11 and 4 times faster in the MIS1 mistuned case, and 17 and 4 times faster in the MIS2 mistuned case. Due to the additional interface DOF in the reduced system, the methods using partial interface modes require more CPU times than the methods using interface modes. In the tuned case, the former methods with Selection P1 are only slightly slower than the latter methods, but they provide much better results. In the mistuned cases, the former methods with Selection P1 are about 3 times slower than the latter methods. Selection P2 requires about 1.5 times more CPU time than Selection P1, but the results are not much better.

The use of the tuned modes in the MIS2 mistuned case in place of the mistuned modes in the MIS1 mistuned case deteriorates significantly the results and does not reduce the CPU times as much as we may expect, since the saving on the CPU times only comes from the model reduction, or more precisely on the computation of the substructure modes and the interface modes or partial interface modes, and not from the solution of the reduced system.

6. Conclusion

Several CMS methods using partial interface modes which allows to reduce the number of interface generalized coordinates and at the same time to keep a few physical displacements in the reduced coupled system have been developed. They are applied on a bladed disk with cyclic symmetry and they are compared with the classical CMS methods and the CMS methods using interface modes. The results obtained with all the CMS methods are in very good agreement with the reference results.

According to the results obtained in this example, the following recommendations can be made:

- if the number of the interface DOF is not an issue, the classical CMS methods give the best results. The free interface methods are recommended since they are the most accurate, although

the fixed interface methods are also easy to implement and they work well with a large range of applications.

- if the number of the interface DOF is too important and has to be reduced, the new CMS methods using partial interface modes are recommended. And even in the case the physical displacements are not needed in the reduced coupled system, it is better to keep some of them and use the partial interface modes rather than the interface modes, since the former are much better concerning the accuracy and the convergence of the results. A small number of the kept interface DOF and the mode selections derived from Rubin's criterion are sufficient to obtain very good results, and the increase of the number of the kept interface DOF or the selected modes do not improve very much the results.
- for the mistuned case, the use of the tuned substructure, interface and partial interface modes in the CMS methods is not recommended, since it deteriorates significantly the results. The use of the mistuned modes provides much better results with only a small additional computational cost.

The development of CMS methods based on the proper orthogonal decomposition [57] is in progress. The future works will consist in using CMS methods for further investigation on mistuned bladed disk systems with non-linearity and aeroelastic coupling.

References

- [1] Admire JR, Tinker ML, Ivey EW. Residual flexibility test method for verification of constrained structural models. *AIAA J* 1994;32(1):170-5.
- [2] Aoyama Yuji, Yagawa Genki. Component mode synthesis for large-scale structural eigenanalysis. *Comput Struct* 2001;79:605-15.
- [3] Bamford RM. A model combination program for dynamic analysis of structures. Tech. memo. 33-290, Jet Propulsion Laboratory, Pasadena, CA; 1967.
- [4] Batailly A, Legrand M, Cartraud P, Pierre C, Lombard J-P. Study of component mode synthesis methods in a rotor-stator interaction case. In: Proceedings of the ASME international design engineering technical conferences and computers and information in engineering conference; 2007.
- [5] Bathe KJ. Finite element procedures. Upper Saddle River [NJ]: Prentice Hall; 1996.
- [6] Benfield WA, Hrudá RF. Vibration analysis of structures by component mode substitution. *AIAA J* 1971;9(7):1255-61.
- [7] Berlioz A, Ferraris G. Utilisation de la sous-structuration en dynamique des rotors. *Matér Méc Electr* 1986(416):30-3.
- [8] Besset S, Jézéquel L. Dynamic substructuring based on a double modal analysis. *ASME J Vib Acoust* 2008;130(1):011008.
- [9] Bladh R, Castanier MP, Pierre C. Component-mode-based reduced order modeling techniques for mistuned bladed disks. Part I: Theoretical models. *ASME J Eng Gas Turb Power* 2001;123(1):89-99.
- [10] Bladh R, Castanier MP, Pierre C. Component-mode-based reduced order modeling techniques for mistuned bladed disks. Part II: Application. *ASME J Eng Gas Turb Power* 2001;123(1):100-8.
- [11] Bouhaddi N, Lombard JP. Improved free-interface substructures representation method. *Comput Struct* 2000;77:269-83.
- [12] Bourquin F. Component mode synthesis and eigenvalues of second order operators: discretization and algorithm. *Modél Math Anal Numér* 1992;26(3):385-423.
- [13] Bourquin F, D'Hennezel F. Intrinsic component mode synthesis and plate vibrations. *Comput Struct* 1992;44(1/2):315-24.
- [14] Bucher ChUA. A modal synthesis method employing physical coordinates, free component modes, and residual flexibilities. *Comput Struct* 1986;22(4):559-64.
- [15] Capiez-Lernout E. Dynamique des Structures Tournantes à Symétrie Cyclique en Présence d'Incertitudes Aléatoires. Application au Désaccordage des Roues Aubagées. PhD thesis, Université de Marne-La-Vallée, France; 2004.
- [16] Choi B-K, Lentz J, Mignolet MP, Rivas-Guerra AJ. Optimization of intentional mistuning patterns for the reduction of the forced response effects of unintentional mistuning: formulation and assessment. *ASME J Eng Gas Turb Power* 2003;125:131-40.
- [17] Corus M, Balmès E, Nicolas O. Using model reduction and data expansion techniques to improve SDM. *Mech Syst Signal Process* 2006;20:1067-89.
- [18] Craig Jr RR. A review of time-domain and frequency-domain component mode synthesis methods. In: Martinez David R, Keith Miller A, editors. Combined experimental/analytical modeling of dynamic structural systems. AMD, ASME, vol. 67. Sandia National Laboratories; 1985. p. 1-30.
- [19] Craig Jr RR, Bampton MCC. Coupling of substructures for dynamic analysis. *AIAA J* 1968;6(7):1313-9.
- [20] Craig Jr, RR, Chang C-J. On the use of attachment modes in substructure coupling for dynamic analysis. In: Proceedings of the AIAA/ASME 18th structures, structural dynamics, and materials conference, vol. B, AIAA paper 77-405; 1977. p. 89-99.
- [21] Craig Jr, RR, Chang C-J. Substructure coupling for dynamic analysis and testing. NASA CR-2781; 1977.
- [22] Crandall SH, Yeh NA. Component mode synthesis of multi-rotor systems. In: Elishakoff I, Irretier H, editors. Refined dynamical theories of beams, plates and shell and their applications. Euromech colloquium 219th, Lectures notes in engineering, vol. 28. Springer-Verlag; 1986. p. 44-55.
- [23] Curnier A. On three modal synthesis variants. *J Sound Vib* 1983;90(4):527-40.
- [24] Davidsson P, Sandberg G. A reduction method for structure-acoustic and poroelastic-acoustic problems using interface-dependent Lanczos vectors. *Comput Method Appl Mech Eng* 2006;195:1933-45.
- [25] de Klerk D, Rixen DJ, Voormeeren SN. General framework for dynamic substructuring: history, review, and classification of techniques. *AIAA J* 2008;46(5):1169-81.
- [26] Engels RC. Convergence improvement for component mode synthesis. *AIAA J* 1992;30(2):490-5.
- [27] Farhat C, Geradin M. On a component mode synthesis method and its application to incompatible substructures. *Comput Struct* 1994;51(5):459-73.
- [28] Farvacque M, Gantenbein F, Gibert RJ, Guilbaud D. Formalisme du programme d'analyse dynamique par sous-structuration OSCAR développé dans le cadre du système CASTEM 2000. Rapport technique, C.E.A.; 1984.
- [29] Flasner H. An orthogonal decomposition approach to modal synthesis. *Int J Numer Method Eng* 1986;23:471-93.
- [30] Ganine V, Legrand M, Pierre C, Michalska H. A reduction technique for mistuned bladed disks with superposition of large geometric mistuning and small model uncertainties. In: Proceedings of the 12th international symposium on transport phenomena and dynamics of rotating machinery, ISROMAC 2008-20158; 2008.
- [31] Geradin M, Rixen D. Mechanical vibrations: theory and applications to structural dynamics. 2nd ed. John Wiley and Sons; 1997.
- [32] Goldman RL. Vibration analysis by dynamic partitioning. *AIAA J* 1969;7(6):1152-4.
- [33] Guyan RJ. Reduction of stiffness and mass matrices. *AIAA J* 1965;3(2):960-1.
- [34] Hassis H. Proposition of a new approach for the substructure method. *J Sound Vib* 2000;234(4):659-68.
- [35] Henry R. Calcul des fréquences et modes des structures répétitives circulaires. *J Méc Appl* 1980;4(1):61-82.
- [36] Hintz RM. Analytical methods in component modal synthesis. *AIAA J* 1975;13(8):1007-16.
- [37] Hou S. Review of modal synthesis techniques and a new approach. *Shock Vib Bull* 1969;40(Part 4):25-39.
- [38] Humar JL, Soucy Y. Hybrid component mode synthesis based on test derived data. *Comput Struct* 1998;67:503-15.
- [39] Hurty WC. Vibrations of structural systems by component mode synthesis. *J Eng Mech Div, Proc Am Soc Civil Eng* 1960;86(EM 4):51-69.
- [40] Hurty WC. Dynamic analysis of structural systems using component modes. *AIAA J* 1965;3(4):678-85.
- [41] Imbert JF. Analyse des Structures par Eléments Finis. Deuxième édition, Cepadue Editions; 1984.
- [42] Jézéquel L. A hybrid method of modal synthesis using vibrations tests. *J Sound Vib* 1985;100(2):191-210.
- [43] Jézéquel L, Tchere ST. A procedure for improving component mode representation in structural dynamics analysis. *J Sound Vib* 1991;144(3):409-19.
- [44] Kubomura K. A theory of substructure modal synthesis. *J Appl Mech* 1982;49:903-9.
- [45] Kuhar EJ, Stahle CV. Dynamic transformation method for modal synthesis. *AIAA J* 1974;12(5):672-8.
- [46] Leung AYT. Dynamic substructure response. *J Sound Vib* 1991;149(1):83-90.
- [47] Li Aiqin, Dowell EH. Modal reduction of mathematical models of biological molecules. *J Comput Phys* 2006;211:262-88.
- [48] Liu W, Ewins DJ. Substructure synthesis via elastic media. *J Sound Vib* 2002;257(2):361-79.
- [49] MacNeal RH. A hybrid method of component mode synthesis. *Comput Struct* 1971;1(4):581-601.
- [50] Martinez DR, Miller AK, Carne TG. Combined experimental/analytical modeling of shell/payload structures. In: Martinez David R, Keith Miller A, editors. Combined experimental/analytical modeling of dynamic structural systems. AMD, ASME, vol. 67. Sandia National Laboratories; 1985. p. 167-94.
- [51] Masson G, Ait Brik B, Cogan S, Bouhaddi N. Component mode synthesis (CMS) based on an enriched Ritz approach for efficient structural optimization. *J Sound Vib* 2006;296:845-60.
- [52] Meirovitch L. Computational methods in structural dynamics. The Netherlands: Sijthoff and Noordhoff; 1980.
- [53] Mignolet MP, Soize C. Nonparametric stochastic modeling of structures with uncertain boundary conditions and uncertain coupling between substructures. In: Proceedings of the 49th AIAA structures, structural dynamics, and material conference, AIAA paper 2008-2291. Chicago [IL]: Schaumburg; 2008.
- [54] Morand H, Ohayon R. Fluid-structure interactions. Wiley; 1995.
- [55] Ohayon R. Reduced models for fluid-structure interaction problems. *Int J Numer Method Eng* 2004;60:139-52.
- [56] Ohayon R, Sampaio R, Soize C. Dynamic substructuring of damped structures using singular value decomposition. *ASME J Appl Mech* 1997;64:292-8.

- [57] Placzek A, Tran D-M, Ohayon R. Hybrid proper orthogonal decomposition formulation for linear structural dynamics. *J Sound Vib* 2008;318:943–64.
- [58] Qiu Ji-Bao, Ying Zu-Guang, Williams FW. Exact modal synthesis techniques using residual constraint modes. *Int J Numer Method Eng* 1997;40:2475–92.
- [59] Rixen D, Farhat C, G eradin M. A two-step two-field hybrid method for the static and dynamic analysis of substructure problems with conforming and non-conforming interfaces. *Comput Method Appl Mech Eng* 1998;154:229–64.
- [60] Rixen DJ. A dual Craig–Bampton method for dynamic substructuring. *J Comput Appl Math* 2004;168:383–91.
- [61] Rubin S. Improved component-mode representation for structural dynamic analysis. *AIAA J* 1975;13(8):995–1006.
- [62] Schott  J-S, Ohayon R. Various modelling levels to represent internal liquid behaviour in the vibration analysis of complex structures. *Comput Method Appl Mech Eng* 2009;198:1913–25.
- [63] Shanmugam A, Padmanabhan C. A fixed-free interface component mode synthesis method for rotordynamics analysis. *J Sound Vib* 2006;297:664–79.
- [64] Shyu W-H, Ma Z-D, Hulbert GM. A new component mode synthesis method: quasi-static mode compensation. *Finite Element Anal Des* 1997;24:271–81.
- [65] Spanos JT, Tsuha WS. Selection of component modes for flexible multibody simulation. *J Guid* 1991;14(2):278–86.
- [66] Suarez LE, Singh MP. Improved fixed interface method for modal synthesis. *AIAA J* 1992;30:2952–8.
- [67] Takewaki Izuru. Inverse component-mode synthesis method for redesign of large structural systems. *Comput Method Appl Mech Eng* 1998;166:201–9.
- [68] Thomas DL. Dynamics of rotationally periodic structures. *Int J Numer Method Eng* 1979;14:81–102.
- [69] Thonon C, G eradin M, Cardonna A, Farhat C. Unification of the impedance and component mode formulations in the assembling of flexible structures. Application to linear systems, vol. 1. Report VA-144, L.T.A.S., Universit  de Li ge; 1995.
- [70] Thonon C, G eradin M, Cardonna A, Jetteur P. Unification of the impedance and component mode formulations in the assembling of flexible structures. Application to nonlinear systems, vol. 2. Report VA-166, L.T.A.S., Universit  de Li ge; 1995.
- [71] Tournour MA, Atalla N, Chiello O, Sgard F. Validation, performance, convergence and application of free interface component mode synthesis. *Comput Struct* 2001;79:1861–76.
- [72] Tran D-M. Component mode synthesis methods using interface modes. Application to structures with cyclic symmetry. *Comput Struct* 2001;79(1):209–22.
- [73] Tran D-M. M ethodes de synth se modale mixtes. *Rev Eur El ments Finis* 1992;1(2):137–79.
- [74] Tran D-M. Hybrid methods of component mode synthesis. In: Actes du forum international a ro elasticit  et dynamique des structures. Strasbourg: AAAF; 1993. p. 911–25.
- [75] Valid R, Ohayon R. Th orie et calcul statique et dynamique des structures   sym tries cycliques. *La Recherche A rospatiale* 1985;4:251–63.
- [76] Wang W, Kirkhope J. Component mode synthesis for multi-shaft rotors with flexible inter-shaft bearings. *J Sound Vib* 1994;173(4):537–55.
- [77] Wang W, Kirkhope J. Component mode synthesis for damped rotor systems with hybrid interfaces. *J Sound Vib* 1994;177(3):393–410.
- [78] Wang W, Kirkhope J. Complex component mode synthesis for damped systems. *J Sound Vib* 1995;181(5):781–800.
- [79] Yan YJ, Cui PL, Hao HN. Vibration mechanism of a mistuned bladed-disk. *J Sound Vib* 2008;317:294–307.
- [80] Zou Chun-Ping, Hua Hong-Xing, Chen Duan-Shi. Modal synthesis method of lateral vibration analysis for rotor-bearing system. *Comput Struct* 2002;80:2537–49.